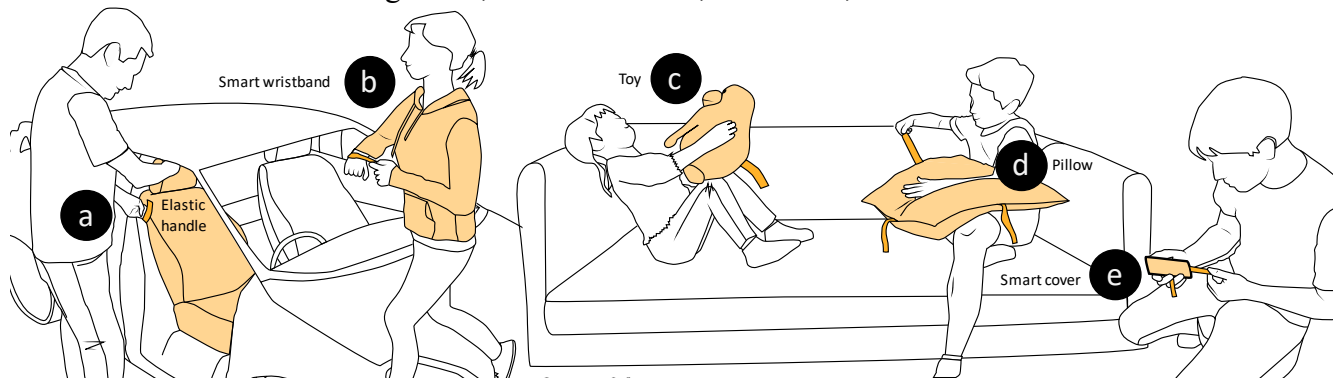


# StretchEBand: Enabling Fabric-based Interactions through Rapid Fabrication of Textile Stretch Sensors

Anita Vogl<sup>1</sup> Patrick Parzer<sup>1</sup> Teo Babic<sup>1</sup> Joanne Leong<sup>1</sup> Alex Olwal<sup>2</sup> Michael Haller<sup>1</sup>

<sup>1</sup> Media Interaction Lab, University of Applied Sciences Upper Austria

<sup>2</sup> Google Inc., Mountain View, California, United States



**Figure 1:** StretchEBand, a textile-based stretch sensor for interacting with a variety of devices. (a) Adjusting car seats, (b) Changing music track during a run, (c) playing with toys, (d) controlling the TV with pillows, (e) and interacting with a smart phone cover.

## ABSTRACT

The increased interest in interactive soft materials, such as smart clothing and responsive furniture, means that there is a need for flexible and deformable electronics. In this paper, we focus on stitch-based elastic sensors, which have the benefit of being manufacturable with textile craft tools that have been used in homes for centuries. We contribute to the understanding of stitch-based stretch sensors through four experiments and one user study that investigate conductive yarns from textile and technical perspectives, and analyze the impact of different stitch types and parameters. The insights informed our design of new stretch-based interaction techniques that emphasize eyes-free or causal interactions. We demonstrate with *StretchEBand* how soft, continuous sensors can be rapidly fabricated with different parameters and capabilities to support interaction with a wide range of performance requirements across wearables, mobile devices, clothing, furniture, and toys.

## Author Keywords

Smart textiles, interactive textiles, stretching sensor, deformation, smart car seat, DIY, fabrication.

## ACM Classification Keywords

H.5.2 User Interfaces: Input devices and strategies; Interaction styles; Haptic I/O.

Permission to make digital or hard copies of all or part of this work for personal or classroom use is granted without fee provided that copies are not made or distributed for profit or commercial advantage and that copies bear this notice and the full citation on the first page. Copyrights for components of this work owned by others than ACM must be honored. Abstracting with credit is permitted. To copy otherwise, or republish, to post on servers or to redistribute to lists, requires prior specific permission and/or a fee. Request permissions from [Permissions@acm.org](mailto:Permissions@acm.org).

CHI 2017, May 06–11, 2017, Denver, CO, USA

© 2017 ACM. ISBN 978-1-4503-4655-9/17/05...\$15.00

DOI: <http://dx.doi.org/10.1145/3025453.3025938>

## INTRODUCTION

We are currently seeing how computation and connectivity is making its way to more and more objects in our lives. Miniaturization, lower cost, and increased power efficiencies will allow electronics to become even more ubiquitous in homes, transportation, and public spaces through embedded technology in furniture, textiles, and other soft objects. It is, however, challenging to equip this integrated technology with appropriate user interfaces (UIs) that can gracefully extend the qualities and capabilities of their contexts without requiring disruptive engineering.

Designers and technologists are therefore developing new types of electronic textiles and smart clothing [7, 15, 24, 29]. By combining textile processing methods with conductive fibers, yarns and fabrics, we can enable a larger space of sensing possibilities. While related work mostly tends to focus on how to implement smart fabric sensors [24], we are mainly interested in *stretch-based* textile sensing technology that can *enhance* or *augment* everyday objects.

In this paper, we present *StretchEBand*, a textile-based stretch sensor, which allows users to interact with a variety of devices in a new way. While we consider the novel form factor and the resulting interaction techniques as the main contributions of this paper, we also present technical novelty in how we leverage stretch sensing for multimodal interaction in different contexts. Building on previous work that utilizes mostly an additional rubber band sensor to enhance flexible bands, we propose a yarn-based approach.

We firstly want to understand the underlying material. Therefore, we analyze, with four experiments, the pros and cons of different yarns and show how yarn can be used in combination with elastic fabrics, and we analyze different stitch properties.

Next, we explore the subjective perception of recognized stretching levels using bands with different elasticities and lengths. We are interested in how elasticity and/or the size influence personal perception of how these sensors behave, and if such factors should be considered in the sensor design. Summarizing, the main contributions of this paper are:

- Analysis and insights needed to fabricate and use a wide array of stitched sensors gained through four experiments and one user study.
- Investigation of conductive yarns from both textile and technical perspectives. We analyze the impact of different stitch types and parameters.
- Five interaction techniques, which arise from combining stretch sensing with touch, pressure, and lift gestures.
- A set of application scenarios that highlight the novel interaction possibilities.
- Analysis of a quantitative evaluation of study participants' reactions and feedback on our interaction techniques and applications, which we hope will help inform future work.

## RELATED WORK

We first review prior work that explores production methods for creating stretch sensors. We then summarize various interaction techniques that illustrate the need for new ways of interacting with small form factor devices.

### Stretch Sensor Materials and Fabrication

Stretch-activated conductive rubber, rubber cord or bands, flex sensors or flexible solar panels [5, 24] or commercially available products (e.g. StretchSense [30]) benefit from their straightforward attachment to most fabrics. However, positioning may affect user comfort when integrated in clothing. Conductive paint [24] as a rapid fabrication method is also dependent on the base structure of the fabric. Elastic conductive fabrics or knitted stainless steel [24] can be seamlessly integrated into fabrics, but require designers to plan ahead and think carefully about positioning and layout; once created, such sensors are difficult to modify. Hence, despite the diverse range of existing techniques for creating stretch-sensors, there lacks an approach for creating stretch-sensors that are comfortable to wear, quick to fabricate, and easy to integrate into existing objects. *StretchEBand* is designed to fill this gap by direct embedment into an existing elastic base material, visible discreteness and scalability to conform to an existing object's form-factor, all without requiring any new layers (i.e. new physical constraints) to be added or imposed on the object.

### Stretch Sensing Using Yarn and Textile

By distinguishing between staple fibers (short pieces of yarn), and filaments (continuous pieces of yarn), we can differentiate between two sensing principles. Staple fibers have gaps between the strands. These gaps close when the yarn is strained, and the resulting touching staple fibers have a larger cross-sectional area than their individual staple fiber strands [27, 28]. Mixed wool (conductive and non-conductive) is used by many researchers [4, 26, 28, 29], with applications ranging from simple stretch detection [29] to the control of audio output [12], as well as, activity-tracking and rehabilitation for the elderly

[4]. In contrast to the sensing principle of staple fibers, the cross-sectional area of a filament-based yarn, decreases when stretched, as the single filaments become longer and thinner. While both principles are applicable for stretch sensing, for the textile processing method of stitching, we chose a thin yarn based on filaments to make the integration as seamless as possible.

### Imprecise and Eyes-Free Interaction Techniques

*Continuous input* enables users to control input with fine granularity. Similar to pressure sensing [18] or folding [15], stretching can be used for continuous input like list scrolling or sliding. The applications can range from music control on a smartwatch, to a seat control in a car, to scrolling through an article on the smartphone. In contrast to discontinuous input, stretching can be used to adjust the speed of navigation.

*Around-Device Interaction* is interesting when users want to act more casually or quickly, as with dismissing a phone call when busy, checking a message when one's hands are wet or dirty, or reading the news when it is cold outside. Furthermore, the screen is less occluded. While Above-Device interactions enable rich 3D input [6, 16], they have limitations, such as, the environment in which they are performed [10]. Stretch-dependent sensors in mobile devices have the potential to extend the interaction space while enabling more casual and less obtrusive interactions.

Wrist-worn devices have smaller form factors that make *touch* difficult, as the input space is limited and emphasizes the *fat finger problem* [25]. On-screen solutions such as Zoomboard [19], which used iterative zooming or Facet [17], which uses multiple displays, support precise interactions, such as text entry. Similar to other approaches [11, 20] involving a touch-sensitive wristband, our stretch-sensitive wristband extends the interaction space of small form factor devices. While previous approaches demonstrate text-entry and pointing or sliding tasks, *StretchEBand* focuses on imprecise interactions, which can happen while users are in motion and want to perform *micro-interactions* [2].






Fabric sensors open new possibilities for *embedding interaction into everyday objects*. Instant UIs demonstrated how a pen or a mug can be used as input devices if other controllers are unavailable [8]. *StretchEBand* follows this principle with integration of stretch sensors into a pillow or a car seat as examples of embedding interaction possibilities into everyday surroundings. Finally, we are highly motivated by the wide range of possible shapes for future computing devices, which we imagine will be as scalable, flexible and transformable as organic life itself [13]. Therefore, we see *StretchEBand* as an example of something that is scalable in fabrication, flexible in attachment, and is transformable with regards to its size, form factor, and material.

## SENSOR DESIGN

To understand how *StretchEBand* is implemented, we performed two experiments to analyze the material properties and relations for different yarns. Both the yarn structure and the base material influence the sensing behavior, given how fabric



strain sensors are formed. The resistance of a given material can be described by the formula  $R = \rho \cdot l/A$ , where  $R$  is the electrical resistance and  $\rho$  is the material resistance, which is constant for each yarn type. The resulting resistance is thus proportional to the length of the yarn ( $l$ ) and inversely proportional to its cross-sectional area ( $A$ ), which depends on the structure and the base material. Staple fiber-based yarns [12, 26, 28, 29] have a negative, linear correlation between stretching and resistance, whereas filament-based yarns have a positive linear correlation [14]. Thus, the longer the yarn, the higher the resistance.

Name	Conductive Thread – 60g	Nm 10/3 Conductive Yarn	High Conductive Silver Plated Nylon Thread	Resistive Thread	Silver Plated Nylon
Manuf. Distributor	Sparkfun Shieldex	Plug and Wear	Shieldex	Plug and Wear	Inventables
Microscope Image					
Yarn Type	Double twine	Triple twine	Double twine	Double twine	Triple twine
Base Yarn	Spinning yarns	Spinning yarns	Spinning yarns	Sleeked filament yarns	Sleeked filament yarns
Structure	Staple fibers	Staple fibers	Staple fibers & Filaments	Filaments	Filaments
Material	100% Stainless steel	80% Polyester 20% Stainless steel	99% Silver	65% Silk 35% Stainless steel	Nylon Silver
Conductivity	Full	Partly	Partly	Partly	Partly
Resistance (per m)	67 $\Omega$ (SD: 3.6%)	410 $\Omega$ (SD: 9%)	900 $\Omega$ (SD: 2.5%)	199 $\Omega$ (SD: 1.2%)	2954 $\Omega$ (SD: 0.5%)

**Table 1: Conductive yarns, the yarn type, the material and the resistance per meter.**

Table 1 shows the differences in structure, conductivity, and base materials for five different yarns we have chosen to analyze in the following four experiments.

### Experiment 1: Yarn Length and Resistance

To measure resistance at our workbench, we fixed the yarn on one end and attached a weight of 60 g at the other end, to avoid tension-based differences. Furthermore, we measured the resistance of the yarn every 10 cm. This procedure was repeated three times per yarn for a total of 45 measurements.

All five yarns provide a positive linear correlation between yarn length and resistance, see Figure 2 (left). *Silver Plated Nylon* has the highest resistance change per measurement step ( $M = 219.5 \Omega / 10 \text{ cm}$ ), while *Conductive Thread – 60 g* has the lowest ( $M = 6.3 \Omega / 10 \text{ cm}$ ).

### Experiment 2: Yarn Tension and Resistance

Next, we investigated how the correlation coefficients between tension and changes in resistance vary across the yarns. We fixed each yarn on one end and attached different weights on the other end. The resistance was measured from 0 cm to 50 cm. We measured five times per yarn for each of the weights, ranging from 50 g to 300 g (in 50 g increments) for a total of 30 measurements.

The staple fiber-based *Conductive Thread – 60 g* and the *Nm 10/3 Conductive Yarn* have a negative correlation between yarn tension and resistance. As the *High Conductive Silver Plated Nylon Thread* is both staple fiber- and filament-based, it shows a positive and then a negative correlation behavior.

The filament-based yarns have a positive correlation, see Figure 2 (right).

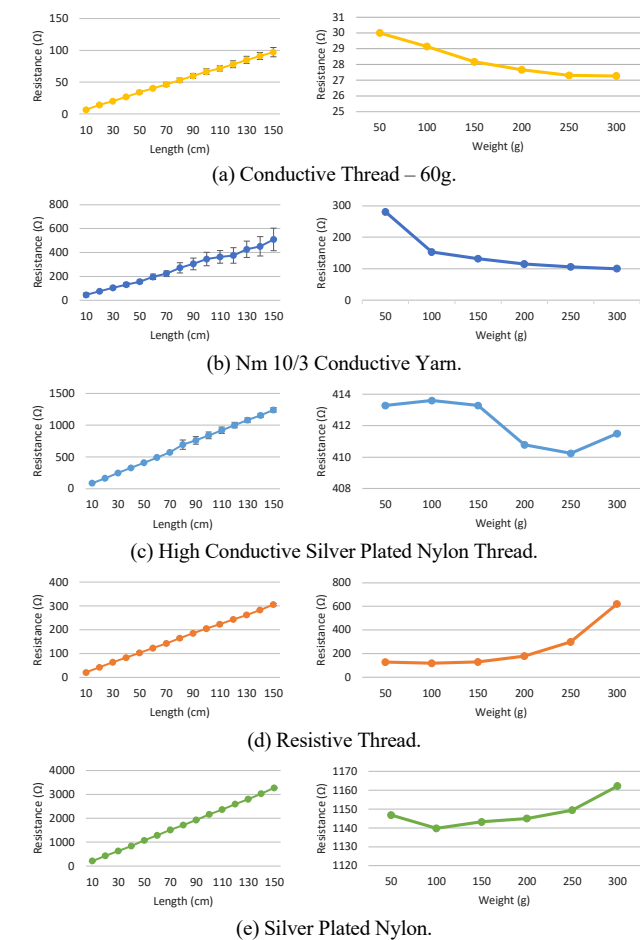


**Figure 2: Changes in resistance ( $\Omega$ ) over different yarn lengths (left) and over different amounts of applied tension (right).**

### Discussion

Based on our observations, we chose to use the *Silver Plated Nylon* in the subsequent experiments. Although this yarn did not lead in all aspects, it had the best balance of the desired properties. (1) Consistent resistance changes over multiple stretch trials: Experiment 1 demonstrates that staple fiber-based yarns have a larger deviation ( $M = 2.86\%$ ,  $SD = 0.27$ ) than filament-based yarns ( $M = 0.91\%$ ,  $SD = 0.14$ ) in an idle state at different lengths, which is explained by its structure (short pieces that touch each other). (2) An approximate monotonic tension-resistance response behavior – the behavior is not perfectly monotonic, but is still more intuitive than that of the *High Conductive Silver Plated Nylon*. (3) Smooth surface and greater tensile strength – in contrast to the *Resistive Thread*, the *Silver Plated Nylon* has a smoother surface and is easier to use in the sewing process. (4) While the absolute resistance values are higher, it still offers a usable range of resistance changes. While the lower resistances of steel-based yarns are usually preferable over the higher resistances of silver-plated yarns, the *Silver Plated Nylon* was still chosen due to its qualities in the first three aspects.

## UNDERSTANDING STITCHES

### Stitch Type

Next, we investigated stretchable two-thread stitches provided by standard sewing machines using different stitch widths and lengths. The terminology of a seam, which is used for the following descriptions and experiments is shown in Figure 3 (left). By applying the unit element model of fabric gauge used for creating knitted stretch sensors [28], we were able to implement different stitching patterns with elastic deformability and repeatability. Therefore, we chose three stitches with these properties, as shown in Figure 3 (right).

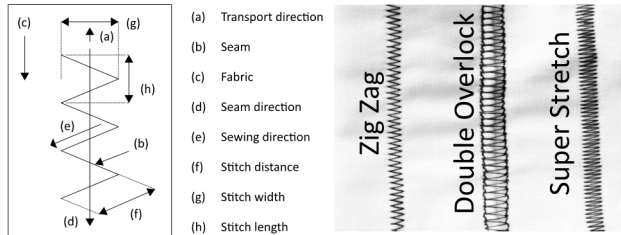


**Figure 3: Terminology of a seam and stitch types: Zig Zag, Double Overlock, and Super Stretch stitch.**

*Zig Zag* has equal stitch distances and is sewn in the seam direction. *Super Stretch* has equal stitch distances, requires more material, and is composed of single stitches that are sewn horizontally or diagonally to the seam direction. *Double Overlock* has unequal stitch distances, while the single stitches are sewn in, against, or diagonal to the seam direction and use more yarn than the other stitching types. We quickly omitted *Straight* stitches after tests showed that the yarn breaks easily when stretched. We tried a lower yarn tension for straight stitches, but due to the yarn being either too loose or too taut, it could not match the continuous resistance change of *Zig Zag*. We excluded *Two Thread Cover* stitches as the looper thread can overlap and easily create short circuits. We also excluded *Three Thread Cover* stitches as they require a special sewing machine.

### Fabric / Substrate

We considered three different substrates: *Elastic Band* (70% Polyester, 30% Elastodiene) – 171% elasticity, *Stretch Garbadine* (95% Polyester, 5% Elastane) – 120% elasticity, and *Cotton Stretch Fabric* (98% Cotton, 2% Elastane) – 125% elasticity. While the elasticity is the maximum amount a substrate is elastic, the stretching amount is the fabric length in relaxed (=100%) versus a defined fully stretched state ( $\geq 100\%$ ) – in the best case the maximum elasticity. We chose the most elastic material, *Elastic Band* (171% elasticity), to allow for greater degrees of stretching in our experiments. This combination of substrate and yarn allowed us to investigate stitch parameters from weak signals to yarn breakage. The results scale up/down to more/less stretchable materials.

### Apparatus & Procedure

For comparable measurements, we sewed a 10 cm seam with a *Bernina B330* [3] on the elastic band by using a stretch needle (strength: 90) with a middle ball tip that is typically used

for highly elastic materials. The top thread was non-conductive cotton, while the bobbin thread was the *Silver Plated Nylon*. So, the bobbin thread was able to float on the back side of the stitch without passing through the fabric substrate [9], which is important for stretching the yarn. Resistance increases with stretching since this is a filament-based yarn. For a consistent connection between the yarn and the measurement system, we sewed conductive fabric (Knit Conductive Fabric – 100% Silver [1]) to the ends of the conductive seam and sewed the *Zig Zag* stitch over that. The ends of the elastic band were sewn to a stable, non-stretchable fabric to keep the tension consistent along the sample width.

Our system enabled stretching along both directions by stretching, stopping and measuring the resistance 37 times  $\times$  10 cycles, while the frequency was constant for all. The total stretching amount was 171%. The resulting resistances were calculated and consolidated for each step, as well as the averages and standard deviations (*SD*), see Figure 4. Average *SD* was  $\sim 10\%$  for the best stretching sample ( $3.3 \times 3.4$  mm).

### Experiment 3: Stitch Types

*Zig Zag*, *Super-Stretch* and *Double Overlock* were evaluated. Only *Zig Zag* has stretch-dependent changes in resistance, as shown in Figure 4 (a); stretched to 171%, its resistance change was about  $58.8 \Omega$ .

### Results

Experiment 3 shows that *Zig Zag* with equally distributed stitches and stitch distances provides the most consistent stretch-sensitive resistance changes. In contrast, variations in sewing direction (cf. *Super-Stretch*) and unequal stitch distance (cf. *Double Overlock*) deliver inconsistent resistance change, where overlapping yarn also often short circuits.

### Experiment 4: Stitch Lengths and Widths

We started with a mid-stitch width and explored different stitch lengths. Figure 4 (b) shows that longer stitches yield higher resistance differences. The 3.4 mm length serves the highest range with  $\sim 122 \Omega$  between no stretching and full stretching. Longer stitches result in yarn breakage, whereas shorter stitches show only small resistance change. We used the estimated stitch length from the previous experiment and explored different stitch widths. Figure 4 (c) depicts that the changes in resulting resistances were higher for samples with narrower widths. We found that a 3.3 mm width serves the highest variation with  $\sim 122 \Omega$ . Narrower stitches were shown to be more prone to breaking under tension, whereas wider stitches resulted in smaller resistance changes.

The drift for the stretching sample with the highest resistance change, while not breaking (stitch length = 3.4 mm, stitch width = 3.3mm) was on average  $\sim 1.09\%$ . Thus, the resulting resistance for a measurement step (e.g. 40% stretch) was on average 1.09% different from the previous cycle.

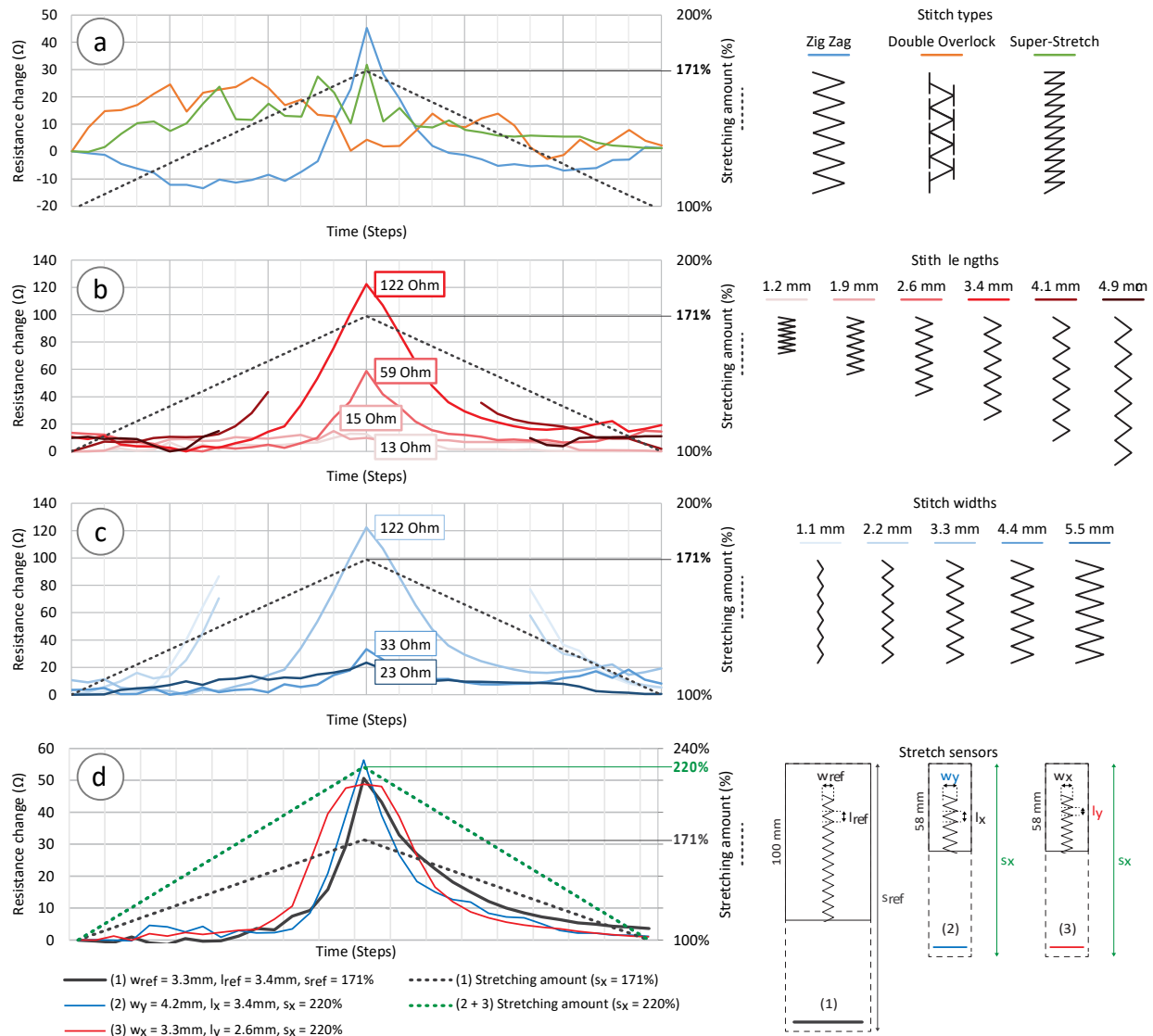


**Figure 4: Resulting changes in resistance (Ω) for varying (a) stitch types, (b) stitch lengths (fixed stitch width = 3.3 mm), (c) stitch widths (fixed stitch length = 3.4 mm), and (d) stretch sensor samples with different elasticities, stitch widths and stitch lengths.**

### Results

The results reflect that long stitches prevent full stretching, as the yarn holds the fabric tightly together and therefore has a risk of tearing. However, stitches that are too short, result in only minor resistance changes, as the yarn is minimally stretched, even when the fabric is fully stretched. Wide stitches result in weak signals as more tension must be applied in the length direction to stretch the yarn. Stitches that are too narrow result in yarn breakage as again the yarn holds the fabric tightly together. Therefore, we conclude:

- *Highly elastic materials need wider stitch widths and/or shorter stitch lengths.*
- *Less elastic materials need narrower stitch widths and/or longer stitch lengths.*

### DESIGN IMPLICATIONS

By considering these effects, we formulate the following formulas for calculating the optimal stitch length and width for a material with a specified elasticity, cf. *Silver Plated Nylon*:

$$l_y(s_x, w_x) = \frac{s_{ref}}{s_x} \cdot \frac{w_x}{w_{ref}} \cdot l_{ref} \quad w_y(s_x, l_x) = \frac{s_x}{s_{ref}} \cdot \frac{l_x}{l_{ref}} \cdot w_{ref},$$

where  $l_y$  is the stitch length to be calculated,  $w_y$  is the stitch width to be calculated,  $w_x$  is the stitch width and  $l_x$  is the stitch length specified by the dimensions of the chosen elastic substrate,  $l_{ref}$  is the reference stitch length (e.g., 3.4 mm),  $w_{ref}$  is the reference stitch width (e.g., 3.3 mm),  $s_{ref}$  is the original maximal stretching amount (in our case 171%) and  $s_x$  is the defined maximal stretching amount of the new material. Therefore, the relationship between a defined stitch width and

calculated stitch length is linear and vice versa. The stitch width is linear to the elasticity and the stitch length is potentially falling by a changing defined maximal stretching amount, as can be seen in Figure 5.

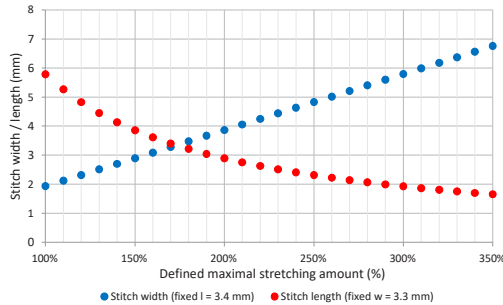


**Figure 5: Ideal stitch width/length for defined maximal stretching amounts.**

### Verification

To verify our proposed formula, we created three samples based on a thinner elastic band with a higher elasticity ( $s_x = 220\%$ ). For the first sample, we used the original settings and the original material ( $s_{ref} = 171\%$ ,  $w_{ref} = 3.3\text{ mm}$ ,  $l_{ref} = 3.4\text{ mm}$ ). Therefore, we stretched the material to an amount of 171%. For the second sample, we varied the stretching amount and the stitch width ( $s_x = 220\%$ ,  $w_y = 4.2\text{ mm}$ ,  $l_x = 3.4\text{ mm}$ ). For the third sample, we used the same stretching amount and changed the stitch length ( $s_x = 220\%$ ,  $w_x = 3.3\text{ mm}$ ,  $l_y = 2.6\text{ mm}$ ). As Figure 4 (d) shows, all three samples have almost the same changes in resistance by applying different stretching amounts. This allows the DIY community to replicate and validate our results and build various stretch sensors based on stitches. The precision and consistency meets our needs, given our focus on casual interaction with wearables, on seats, or with toys, as illustrated in our prototype applications.

### EVALUATION: INFLUENCES FOR THE DESIGN

An empirical study was conducted to understand the influence of sensor length, elasticity of the base material and the perception of stretching levels. We neglected the aspect of easy integration and focused here on robustness. Therefore, we used the base substrate with a rubber chord sensor attached, connected by snap buttons, to keep the setup as stable as possible.

### Participants

12 unpaid volunteers (8 female), 23–36 years old ( $\bar{x} = 30$ ,  $SD = 3.8$ ) were recruited from a partner company and a local university. One participant was left-handed.

### Methodology

The study was conducted in a quiet room with the stretching sensor setup and a screen in front of the participant. To get comparable data, we analyzed and calibrated each sensor.

### Design

We used the stretching sensor and varied it with two different length sizes and two base materials with different elasticities.

The study used a  $2$  (sensor lengths)  $\times 2$  (elasticities)  $\times 3$  (number of stretching levels) within-subjects factorial design with the following factors:

- Sensor length: 8 cm, 10 cm,
- Elasticity: 200%, 250%, and
- Stretching level (granularity): 2, 4, 5.

Participants were asked to stretch the sensor to a specific percentage amount between *Two levels* (50% / 100%), *Four levels* (25% / 50% / 75% / 100%), and *Five levels* (20% / 40% / 60% / 80% / 100%), where the target percentage was shown in the center of the screen. Participants did not get further visual feedback during the stretching activity (see Figure 6 (2)). In contrast to partial visual feedback [21], this simulates an eyes-free condition, where feedback is not visually given (e.g., car seat movement, auditory feedback while running). When participants thought that they had reached the target level (see Figure 6 (3-6)) or were within the correct range, they pressed a foot pedal. They started the next trial by pressing the foot pedal. Overall, we had 1,440 trials. The four combinations of sensor length and elasticity were Latin-square counter-balanced between the participants.

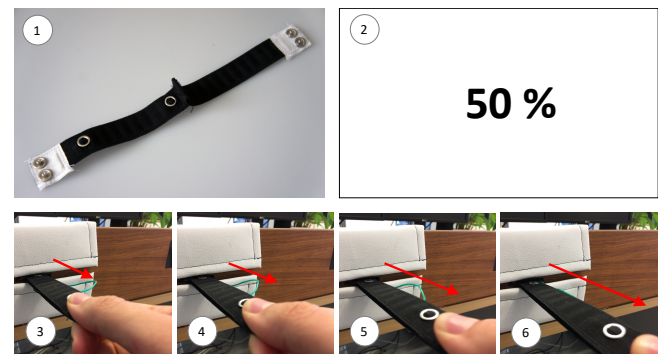


**Figure 6: (1) The stretch sensor, (2) a sample instruction screen given during the user study, (3–6) and one participant in action during the stretching activity in the 4-level condition.**

Stretching granularity was presented in an ascending order for all participants. Ten stretching levels were pre-defined for each stretching granularity block and randomized for each of the participants. Once a participant stretched the sensor, the stretching length was normalized according the calibration and then further compared to the recorded sample. To suppress sensor jitter, we added an additional band-stop filter.

During the experiment, we recorded the completion time, error, error distance, and number of crossings. The completion time was the total time used by the participants to stretch the sensor accordingly until the target had been selected. The number of crossings is the number of times the cursor (not visible to the participant) crosses the target, see Figure 6 (2). The error is the number of times participants selected a location which was not the specified target. Each trial was successfully completed only if participants pressed the foot pedal when they were within the range of the presented stretching level.



## Quantitative Results

Error rates and trial completion times were analyzed using a repeated measures ANOVA ( $\alpha = 0.05$ ) separately for each level of complexity. The Greenhouse-Geisser correction was used if the assumption of sphericity was violated. Post-hoc analyses on the main effects were conducted, consisting of paired-samples t-tests with family-wise error rate controlled across the test using Holms sequential Bonferroni approach.

For all bar charts, the error bars indicate the range of two standard errors of the mean (above and below the mean). Table 2 provides an overview of the completion time, the error distances and the number of crossings for each of the conditions.

Sensor length / Elasticity	Completion time (s)		Error distance (mm)		Number of crossings	
	$\bar{x}$	SD	$\bar{x}$	SD	$\bar{x}$	SD
Long length	1.86	0.86	19.22	13.31	1.02	1.24
Short length	1.82	0.77	18.82	12.35	0.96	1.22
High elasticity	1.94	0.82	20.61	13.53	0.95	1.20
Low elasticity	1.74	0.79	17.43	11.92	1.02	1.26

**Table 2: Completion time, error distance, number of crossings.**

### Completion Time

Figure 7 (left) shows that participants were able to complete the task with the low elastic material significantly faster than with the high elastic material ( $F_{1,1172} = 17.215, p < .001$ ).

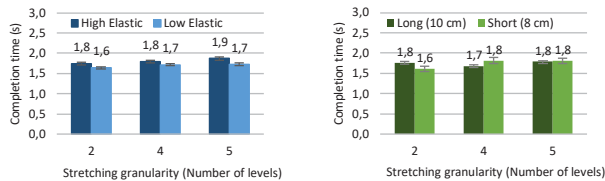


**Figure 7: Mean completion times with different elasticities and lengths.**

Participants were faster with the less sensitive material, but no significant differences between short and long samples were found. The higher the stretching granularity, the faster participants completed the task. For the two, participants were significantly faster than for the five sensing levels ( $F_{2,1171} = 4.814, p < .012$ ) and in the four, participants were also significantly faster than for the five sensing levels ( $F_{2,1171} = 4.814, p < .041$ ). Participants stated that the estimation of stretching length was hard. Not surprisingly, the two-level condition was the easiest to perform.

### Error distance

The error distance was significantly higher with the high than with the low elastic material ( $F_{1,554} = 8.632, p = .003$ ). This again means that materials with higher sensitivity are harder to control. Length had no influence on the error distance.

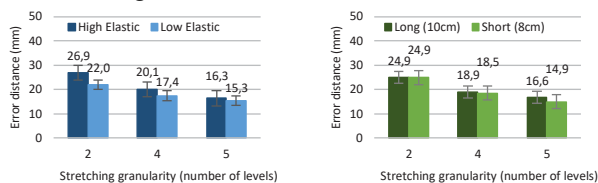


**Figure 8: Mean error distances for elasticities and lengths.**

As Figure 8 shows, the error distance did significantly decrease with the number of sensing levels ( $F_{2,553} = 22.456, p < .001$ ).

.001). Significant differences can be found between two and four ( $p < .001$ ) and two and five sensing levels ( $p < .001$ ). This is a logical consequence as the difference between the two levels in the two-level condition is much bigger than the difference between the different levels in the four or five level condition.

### Number of crossings

We found no significant differences in the number of crossings between the materials or the lengths, cf. Figure 9.

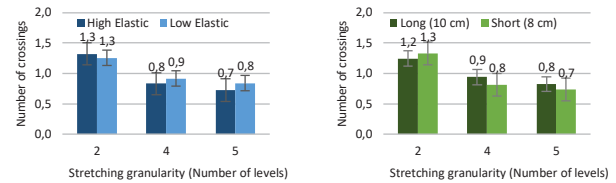
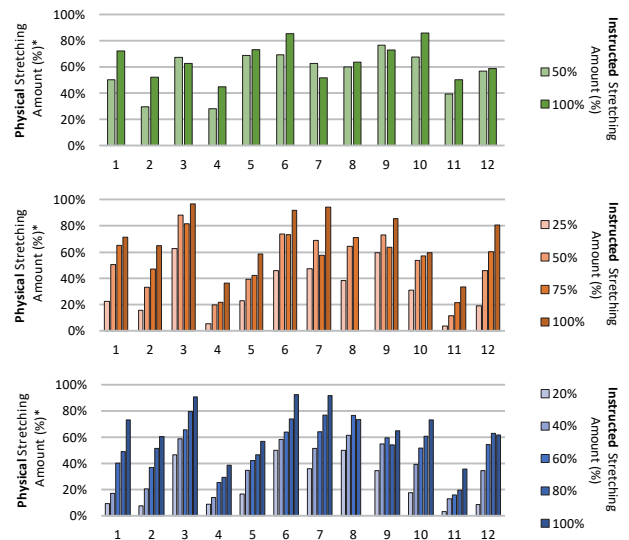


**Figure 9: Mean number of crossings for different elasticities and lengths.**

Post-hoc comparisons of the number of sensing levels showed that targets in the four- ( $p = .012$ ) or five-level condition ( $p < .001$ ) had significantly fewer crossings than in the two-level condition ( $F_{1,1171} = 10.414, p < .001$ ).

### Sensing levels

Our goal was to find out if users could control different stretching levels without any feedback based on their own perception. As depicted in Figure 10, the stretching sensation is highly depending on the individual participant [22].



\* normalized value (0 = relaxed, 100 = full possible stretch) across all 4 stretching samples (2 sensor lengths x 2 elasticities)

**Figure 10: Mean stretching amount for two / four / five-level condition.**

These large differences are a drawback while offering no visual feedback. Pre-defined thresholds would not work for different participants. Therefore, we extracted user-dependent boundaries for the stretching levels from all trials by fitting thresholds between the average stretching level values for each of the participants in each of the three-level conditions separately. Figure 11 presents the mean accuracies for the two-, four-, and five-level condition. The accuracy was high for the two-level condition ( $M = 75\%, SD = 0.28$ ), for the four- ( $M =$



79%,  $SD = 0.25$ ), and for the five-level condition ( $M = 82\%$ ,  $SD = 0.22$ ). The accuracy was significantly better for five than for two levels ( $F_{2,1219} = 7.209$ ,  $p = .001$ ). Especially the accuracies for low stretching amounts (20% / 40%) were high. As Figure 11 reflects, the accuracy decreases with the stretching amount in all three conditions. This indicates that performing light stretches is much easier than stretching to larger amounts.

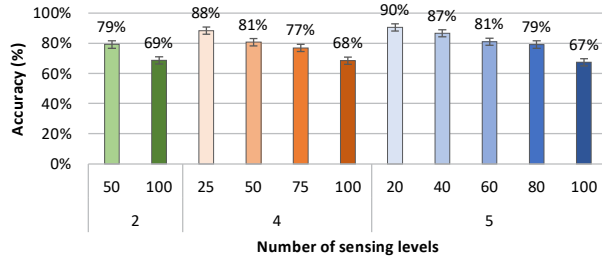


Figure 11: Mean accuracy for two / four / five-level condition.

Therefore, it could be interesting to map more stretching levels to the first part of the sensing range. Contrarily, the error rate was highest for four levels (32%), followed by five levels (30%) and two levels (21%). For two levels, most errors occurred for strong stretching (27%) in contrast to light stretching (17%). In the four-level condition, most errors occurred in the medium stretching conditions (42–47%), followed by light stretching (16%) and strong stretching (11%).

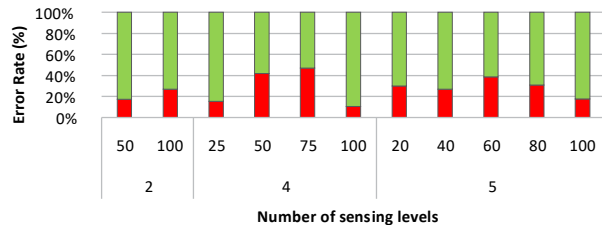


Figure 12: Error rates for two, four and five stretching levels.

A similar pattern was found for the five-level condition, as most errors occurred in the medium stretching conditions (27–39%), followed by light stretching (30%) and strong stretching (18%). Thus, accurately applying a medium amount of stretching is much harder than applying a light or strong stretch (see Figure 12).

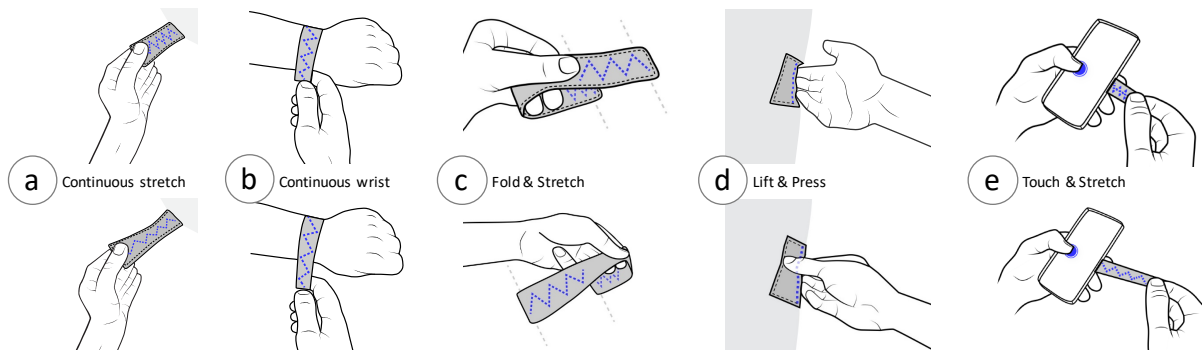


Figure 13: (a) Continuous stretch input for zooming / scrolling, (b) continuous wrist input for interacting in motion, (c) fold & stretch and (d) lift & press for directional input, and (e) touch & stretch for hybrid interaction.

Summarizing, four to five stretching levels can be distinguished, less elastic materials (e.g. stiffer materials) allows easier control in eyes-free conditions, while sensor-length has no impact on the performance.

## INTERACTION TECHNIQUES

The availability of such a stretch-based sensor gives rise to a suite of new gestures which we describe in the following sections, as shown in Figure 13. Later in this paper, the implemented interaction techniques will be showcased in the context of fully working application scenarios.

### Continuous Stretch Input

Given the flexibility of the input sensor, we enable *continuous stretch input*, wherever continuous interaction is required (e.g., zooming a map, scrolling through a list of contacts, controlling a car seat's position). During the discussion with participants after the user study, we found that users appreciated continuous stretch input and found it convenient to control the speed of interaction by stretching the sensor accordingly.

### Continuous Wrist Input

Similarly, the *continuous wrist input* enables integrated interaction with wearable devices in the form of a wristband. By simply pulling the band on the arm, users can quickly and continuously trigger actions.

### Fold & Stretch

While the continuous input modalities are based on a single-step interaction approach with the sensor, the *fold & stretch* metaphor is based on two steps, which happen almost simultaneously: folding *and* stretching. Thus, users fold the sensor and stretch it, along the folding direction.

### Lift & Press

In contrast to the previous interaction techniques, Lift & Press is designed for interactions, where the sensor is to be embedded into an existing textile (e.g. as a handle for a car seat). Similar to a car door handle, users have to trigger the sensor by lifting the elastic band with the fingers (*lift*). On the other side, the sensor is also able to detect subtle touches by the deformation of the stitch-based yarn (*press*), which triggers the opposite action.

### Touch & Stretch

Finally, *touch & stretch* describes a multimodal interaction, where users combine touches with a stretch-gesture on a display. Our implementation has the sensor attached on the back of a smart device.

### APPLICATION EXAMPLES

In this section and in the supplementary video, we present a number of novel application scenarios. They show the benefits of our stretching sensor when combined with different devices, ranging from smartphone covers to interactive car seats. The applications were informed by feedback during the user study.

#### Smartphone Case/Cover

We see interesting potential in expanding smart phone interaction for around-the-device interaction [6] to overcome the *fat-finger problem* [23], by augmenting a protective textile cover.



Figure 14: (1–2) Users can switch between the contacts without cluttering the screen, but also (3–4) pan & zoom into maps efficiently by using a bi-manual approach.

In this application, the stretch sensors are used as an independent input, but they can also be used in combination with the usual touchscreen input. For clarity, Figure 14 shows the stretch sensor without the rest of the cover.

Concretely, we implemented three applications for the smartphone cover:

- *Scrolling*: Here, we enable scrolling down/up in lists by mapping scroll speed to applied pull-force. Therefore, we set a threshold and scrolled by combining the applied pull force with a fixed velocity. *StretchEBand*'s off-screen input avoids occluding screen content, e.g., when scrolling through contacts lists. When the desired contact is in view, the user can tap on the touch screen to select.
- *Application Switching*: The elastic band can be used for changing applications, or returning to a previous state of an application (back/return key).
- *Multimodal Zooming*: We also enable multimodal interaction with the touch screen and stretch sensor. While touching a location, users can stretch in a direction to zoom into the map. Similarly, different gestures can be used to continuously pan (touch) and tilt (stretch-bottom) and rotate (stretch-right) in a 3D map application.

### Smart Wristband

*StretchEBand* can either be used independently, or for hybrid interaction. For instance, it can be used to complement common touch screen interactions.



Figure 15: Switching between tracks in a clutter-free manner.

We see the potential in the combination with smaller devices, such as smart watches, to overcome the limited input space for touch-screen interaction and buttons (e.g., fitness trackers) and to offer imprecise gestures, e.g., while users are interacting with the device during motion (e.g., walking, running, biking). This is particularly relevant for micro interactions [2], such as controlling a stopwatch or music player while running, cf. Figure 15.

### Elastic Handles for Adjusting Car Seats

Next, we implemented three applications for car seat control, as illustrated in Figure 16.



Figure 16: Adjusting the car seat position by stretching the *StretchEBand* sensor.

The overall idea was to enable direct manipulation with soft controls that can be integrated with the existing fabric, and thus replace current rigid buttons, which are currently used to, e.g., adjust car seats. The seat forward and backward control could, e.g., be implemented using the *continuous input*, cf. Figure 16 (1), or the *fold & stretch* interaction technique, cf. Figure 16 (2a, 2b). Both techniques could be more convenient than finding a corresponding side-button. In three-doored cars with fully electronically adjustable seats, there are often two dedicated buttons that tilt the front seat forward for entering the back seat. Here, we implemented the *lift & push* gesture to allow passengers to move the seat forward, cf. Figure 16 (3).

### Stretchy Pillow & Toys

The use of a stitch-based approach enables us to augment interface-less objects with *StretchEBand*, such as pillows and toys (see Figure 17) with minimal engineering.

An enhanced pillow makes it possible to scroll through a picture gallery displayed on a TV, whereas integration into the tail of a stuffed animal affects its mood. In both examples, we are utilizing the possibility to vary the amount of stretching in both directions for a smooth and natural manipulation of linear parameters.

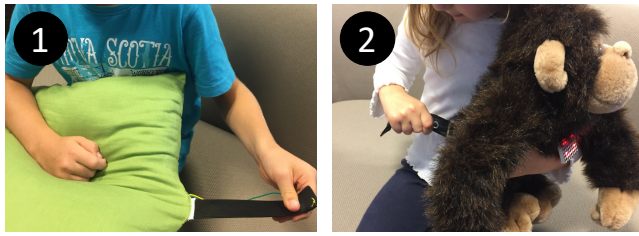


**Figure 17: SketchEBand enhancing everyday objects, e.g. pillows (1) and toys (2).**

### USER FEEDBACK ON SKETCHEBAND

We conducted another study to gather feedback from participants on our implemented *StretchEBand* applications to learn from initial user reactions and comments with a special focus on the proposed interaction techniques.

#### Participants

We recruited 8 participants (4 female), 25–40 years old ( $\bar{x}=32$ ,  $SD=5.5$ ). Five participants were from the local university and three were young professionals.

#### Procedure

We demonstrated the different application scenarios and asked the participants during the 30-minute study to provide critical feedback, focusing on the simplicity and usefulness. All the participants had the possibility to try the demos as long as they wanted.

#### Results

Overall, participants liked the lightweight interaction and the simplicity of how we enhanced everyday object with a smart elastic band. Figure 18 provides an overview of the subjective rankings, including both the interaction techniques, as well as, the applications.

Participants liked the idea of attaching a smart textile cover at the back of the smartphone and to have an additional input modality. Especially, the multi-modal interaction, the combination of touch and stretch, was appreciated by many participants, because it gave them the possibility to zoom in and out very quickly, without occluding the map. All participants found the smooth transition between 2D and 3D (using the *continuous stretch input* for tilting) to be a clever idea. Similarly, they also appreciated the bi-manual interaction. Two participants (*P1*, *P5*) found the cover idea very nice and proposed an updated version, where the cover should be used as a front cover. Once opened, *StretchEBand* could be used as described in this paper. By having this design change, the cover would have a better functionality and protect the screen of the phone. Participants also liked the control of a smart watch with the elastic wristband, because they found that the fat-finger problem was a critical limitation for current devices. Moreover, they agreed that using this while running was a good use case.

Next, all participants enjoyed adjusting the car seat with the embedded bands. Especially, the integration into a car seat was noticed to be “very innovative” (*P4*). None of the participants had difficulties learning the three proposed input techniques. Users mostly liked the *reachability* and *the mapping between*

*the gesture and the resulting action* (*P3*). Moreover, three participants found it “very smart to change the final car seat position so quickly” (*P3*, *P4*, *P8*). Finally, the combination with everyday objects and the enhancement of toys and pillows for controlling the TV was also recognized to be a nice idea with interesting potential for future work.

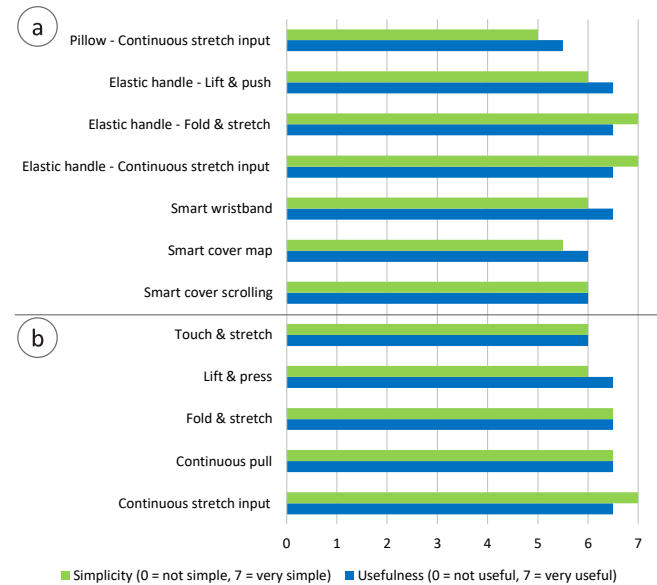


**Figure 18: Subjective rankings of (a) applications and (b) interaction techniques show an overall positive reaction.**

### CONCLUSION & FUTURE WORK

In this paper, we introduced a stitch-based stretch sensor and a systematic evaluation of how stitching parameters relate to sensing properties. We performed four experiments on the influence of yarn structure and stitching properties for stitch-based stretch sensors. The experiments and the additional user study served as a base for the design and implementation of *StretchEBand*. We demonstrated several interaction techniques and application capabilities, and highlighted how stretch sensing can be combined with existing gestures (e.g. touch) in novel ways. The range of applications suggests a rich design space for researchers and practitioners to explore in the future.

For future work, we are mainly interested in improving the robustness, as well as, the reliability of the sensor. Further, we are currently working on a more advanced e-textile. This new fabric will also be able to sense stretching gestures as well as pressure input and will consequently open up a new range of applications, including e-textile covers for sensing socks, prostheses, car seats, and furniture.

### ACKNOWLEDGMENTS

This research received funding from the European Union, 7th Framework Programme FP7/2007-2013 under grant agreement No 611104, and partial funding support from NCBiR, FWF, SNSF, ANR, and FNR in the framework of the ERA-NET CHIST-ERA II (eGlasses).

## REFERENCES

1. Adafruit Knit Conductive Fabric - Silver 20cm square. <http://www.adafruit.com/products/1167>. Accessed on 24-Sep-2015.
2. Ashbrook, D. L. Enabling mobile microinteractions. Georgia Institute of Technology, Atlanta, GA, USA. 2010.
3. Bernina B330. <http://www.bernina.com/en-US/Products-US/BERNINA-products/Sewing-Quilting-and-Embroidery/BERNINA-3-Series/BERNINA-330>. Accessed on 24-Sep-2015.
4. Ten Bhömer, M. and Van Dongen, P. Vigour. *Interactions*. vol. 21, no. 5. pp. 12–13.
5. Buechley, L. SensorMania - Notes from e-Fashion day2008. <http://www.mediamatic.net/36637/en/sensormaniamania>. Accessed on 23-Sep-2015.
6. Butler, A., Izadi, S., and Hodges, S. SideSight: multi-“touch” interaction around small devices. *UIST*. 2008. pp. 201–204.
7. Castano, L. M. and Flatau, A. B. Smart fabric sensors and e-textile technologies: a review. *Smart Mater. Struct.* vol. 23, no. 5. May 2014.
8. Corsten, C., Avellino, I., Möllers, M., and Borchers, J. Instant user interfaces: repurposing everyday objects as input devices. *ITS*. 2013. pp. 71–80.
9. Dunne, L. E., Bibeau, K., Mulligan, L., Frith, A., and Simon, C. Multi-layer e-textile circuits. *UbiComp*. 2012. pp. 649–650.
10. Freeman, E., Brewster, S., and Lantz, V. Towards usable and acceptable above-device interactions. *MobileHCI*. 2014. pp. 459–464.
11. Funk, M., Sahami, A., Henze, N., and Schmidt, A. Using a touch-sensitive wristband for text entry on smart watches. *CHI EA*. 2014. pp. 2305–2310.
12. Glazzard, M. and Kettley, S. Knitted stretch sensors for sound output. *TEI*. 2010. pp. 391–392.
13. Holman, D. and Vertegaal, R. Organic user interfaces: designing computers in any way, shape or form. *Commun. ACM*. vol. 51, no. 6. Jun. 2008. pp. 48–55.
14. Huang, C.-T., Tang, C.-F., Lee, M.-C., and Chang, S.-H. Parametric design of yarn-based piezoresistive sensors for smart textiles. *Sensors Actuators A Phys.* vol. 148, no. 1. Nov. 2008. pp. 10–15.
15. Karrer, T., Wittenhagen, M., Lichtschlag, L., Heller, F., and Borchers, J. Pinstripe: eyes-free continuous input on interactive clothing. *CHI*. 2011. pp. 1313–1322.
16. Kratz, S. and Rohs, M. Hoverflow: exploring around-device interaction with IR distance sensors. *MobileHCI*. 2009. no. 42.
17. Lyons, K., Nguyen, D., Ashbrook, D., and White, S. Facet: a multi-segment wrist worn system. *UIST*. 2012. pp. 123–130.
18. Meyer, J., Arnrich, B., Schumm, J., and Troster, G. Design and Modeling of a Textile Pressure Sensor for Sitting Posture Classification. *IEEE Sens. J.* vol. 10, no. 8. Aug. 2010. pp. 1391–1398.
19. Oney, S., Harrison, C., Ogan, A., and Wiese, J. ZoomBoard: a diminutive qwerty soft keyboard using iterative zooming for ultra-small devices. *CHI*. 2013. pp. 2799–2802.
20. Perrault, S. T., Lecolinet, E., Eagan, J., and Guiard, Y. Watchit: simple gestures and eyes-free interaction for wristwatches and bracelets. *CHI*. 2013. p. 1451.
21. Ramos, G., Boulos, M., and Balakrishnan, R. Pressure widgets. *CHI*. 2004. pp. 487–494.
22. Rendl, C., Greindl, P., Probst, K., Behrens, M., and Haller, M. Presstures: exploring pressure-sensitive multi-touch gestures on trackpads. *CHI*. 2014. pp. 431–434.
23. Riek, K. A., Rogers, Y., and Connelley, K. H. Fat Finger Worries: How Older and Younger Users Physically Interact with PDAs. *INTERACT*. 2005. pp. 267–280.
24. Satomi, M. and Perner-Wilson, H. KOBAKANT. How to get what you want. <http://www.kobakant.at/DIY/?cat=26>. Accessed on 23-Sep-2015.
25. Schmidt, D., Seifert, J., Rukzio, E., and Gellersen, H. A cross-device interaction style for mobiles and surfaces. *DIS*. 2012. pp. 318–327.
26. Wijesiriwardana, R., Dias, T., and Mukhopadhyay, S. Resistive fibre-meshed transducers. *ISWC*. 2003. p. 200.
27. Yoshikai, T., Fukushima, H., Hayashi, M., and Inaba, M. Development of soft stretchable knit sensor for humanoids’ whole-body tactile sensibility. *HUMANOIDS*. 2009. pp. 624–631.
28. Zhang, H., Tao, X., Yu, T., and Wang, S. Conductive knitted fabric as large-strain gauge under high temperature. *Sensors Actuators A Phys.* vol. 126, no. 1. 2006. pp. 129–140.
29. Buechley, L., Peppler, K., Eisenberg, M., and Kafai, Y., Eds. Textile Messages: Dispatches From the World of E-Textiles and Education. 2nd ed. Peter Lang. 2013.
30. Stretch Sense. <https://stretchsense.com/>. Accessed on 29-Dec-2016.